The LERIX User Facility

G.T. Seidler[1], T.T. Fister[1], J.O. Cross[2], and K.P. Nagle[1]

1. University of Washington, Seattle, Washington 98105
2. Argonne National Laboratory, Argonne, IL 60439

Abstract. We describe the lower energy resolution inelastic x-ray scattering (LERIX) spectrometer, located at sector 20 PNC-XOR of the Advanced Photon Source. This instrument, which is now available to general users, is the first user facility optimized for high throughput measurements of momentum transfer dependent nonresonant inelastic x-ray scattering (NRIXS) from the core shell electrons of relatively light elements or the less-tightly bound electrons of heavier elements. By means of example, we present new NRIXS measurements of the near-edge structure for the *L*-edges of Al and the *K*-edge in Si.

Keywords: nonresonant x-ray Raman scattering, x-ray absorption fine structure, x-ray spectrometer.
PACS: 61.10.Ht, 61.20.-p, 61.66.Bi, 71.15.Qe, 61.43Fs, 07.85.Qe

INTRODUCTION

Nonresonant inelastic x-ray scattering (NRIXS) measures the double-differential cross section

$$\frac{d^2\sigma}{d\omega d\Omega} = \left(\frac{d\sigma}{d\Omega}\right)_{Th} S(\mathbf{q},\omega) = \left(\frac{d\sigma}{d\Omega}\right)_{Th} \sum_f \left|\langle f \left| e^{i\mathbf{q}\cdot\mathbf{r}} \right| i\rangle\right|^2 \delta(E_f - E_i - \hbar\omega), \quad (1),$$

where $S(\mathbf{q},\omega)$ is the dynamic structure factor, $(d\sigma/d\Omega)_{Th}$ is the Thomson differential cross section, i and f refer to the initial and final states, respectively, and $\mathbf{r}$ is the position relative to the initial state. It is important to note that $\hbar\omega$ is not the energy of the incident photon, but is instead the difference in energy between the scattered photon ($\hbar\omega_2$) and incident photon ($\hbar\omega_1$). Low-energy excitations can be probed nonresonantly using high-energy incident radiation, i.e., the incident photon energy is decoupled from the energy scale of the physics being studied.

By contrast, the x-ray absorption coefficient is

$$\mu = \sum_f \frac{4\pi^2 e^2}{m^2 c\omega_1 n} \left|\langle f \left| \hat{\varepsilon}\cdot\vec{r} \right| 0\rangle\right|^2 \delta(E_f - E_0 - \hbar\omega_1), \quad (2)$$

and x-ray absorption fine structure (XAFS) measurements require that the incident photon energy be scanned through the binding energy for the relevant initial state. This distinction is important because, in the limit of sufficiently small q,

$$S(\mathbf{q},\omega) \simeq q^2 \sum_f \left|\langle f \left| \hat{q}\cdot\mathbf{r} \right| i\rangle\right|^2 \delta(E_f - E_i - \hbar\omega) \quad (3)$$

so that XAFS with incident photon energy $\hbar\omega_1$ and NRIXS at low q with energy loss $\hbar\omega = \hbar\omega_1$ probe essentially the same transition matrix element for the same initial states, i.e., core shells electrons. NRIXS at low q provides an alternative to UV or soft x-ray absorption measurements [1-25]. However, at larger q the equivalence of the two techniques breaks down, and NRIXS will include nondipolar transitions, thus providing a new window on the symmetry of the possible final states for the photoelectron [14,18,23,26-28].

Here, we summarize the design, capabilities, and range of applications of the lower energy resolution inelastic x-ray scattering (LERIX) spectrometer [28]. LERIX is designed to enable rapid measurements of q-dependent NRIXS for initial state orbitals with binding energies from 10 eV to as much as 2000 eV. The LERIX spectrometer is part of the sector 20 PNC-XOR user facility at the Advanced Photon Source, and beamtime may be requested through the general user program.

EXPERIMENTAL

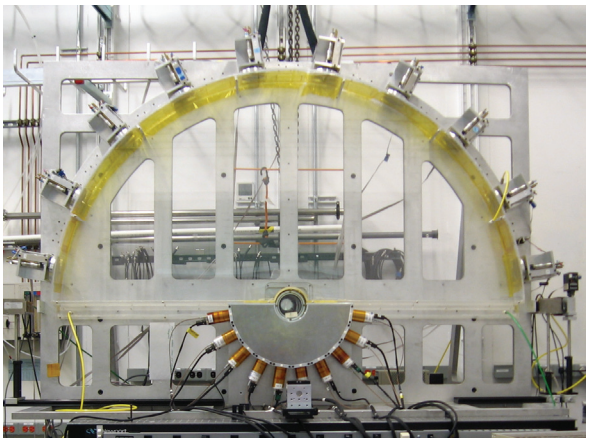

FIGURE 1. The LERIX spectrometer. The incident beam enters from the right. The ten analyzer tilt modules each hold a 4-cm diameter spherically bent Si crystal located ~1m from the sample position. Each analyzer is paired in a near-backscatter arrangement with an independent detector. The analyzers collect radiation from the sample having q = 0.8, 2.4, 3.9, 5.3, 6.6, 7.7, 8.6, 9.3, 9.8, and 10.1 Å^{-1}.

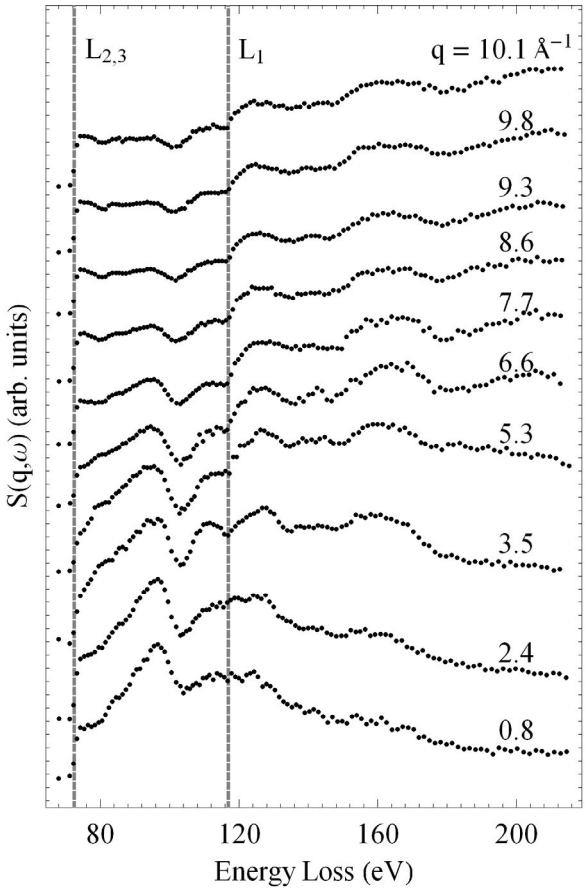

FIGURE 2: Room temperature NRIXS measurements of the Al $L_{2,3}$- and L_1-edges.

Energy loss measurements are achieved through the inverse scanning mode. Each of the ten spherically bent Si analyzers (see Fig. 1) is adjusted so that ~9889 eV radiation is elastically scattered into one of ten corresponding scintillation detectors. The energy of the incident radiation is then scanned through the sum of the elastic scattering energy of the analyzers and the binding energy of the relevant initial state orbital.

The Rowland circle for each analyzer is perpendicular to the vertical scattering plane. Under normal working conditions with an incident photon energy of 10 keV at 20-ID, the overall energy resolution limited by the Si 111 double monochromator to 1.3 eV. The incident flux is ~5 x 10^{12} photons/s. The energy resolution can be improved to 0.8 eV when working instead at lower incident photon energy to access the 333 reflection of the Si analyzers, at some cost in flux and q range.

The LERIX sample space is a 20 cm diameter He-filled load lock. This large sample space allows for a wide range of apparatus to modify the sample environment. A 100 K cryostat, 800 K vacuum furnace, and liquid flow cell have already been designed and are in commissioning for future availability to general users. A more detailed discussion of the design and operation of LERIX has been presented elsewhere [28].

RESULTS AND DISCUSSION

During commissioning studies LERIX has already demonstrated good ease of use and a wide range of applications. LERIX users have had no difficulty measuring such disparate phenomenon as: the near edge structures of the *K*-edge of pure Si; the Sm *O*-edge and B *K*-edge in SmB_6; the Li and C *K*-edges in LiC_6; the O *K*-edge in numerous transition metal oxides; the B *K*-edge in numerous borate minerals; the B and C *K*-edges in the three isomers of the $C_2B_{10}H_{12}$ carborane molecule; the Mg *K*-, *L*-, and *M*-edges and O *K*- and *L*-edges in MgO; and also the extended oscillations for the *L*-edges of pure Mg and Al.

In Fig. 2, to demonstrate the efficiency of LERIX for q-dependent measurements, we present measurements of $S(q,\omega)$ for Al. The extended oscillations for the same sample at T = 100 K are analyzed elsewhere [27]. The valence Compton scattering has been modeled in a Bayesian context, following recent developments in XAFS analysis [29]. The spectra show a rich variation with q, including most notably the strong appearance of the L_1-edge at intermediate q.

In addition to enabling q-dependent measurements of edges with relatively low binding energies, the large solid angle and very low stray background of LERIX

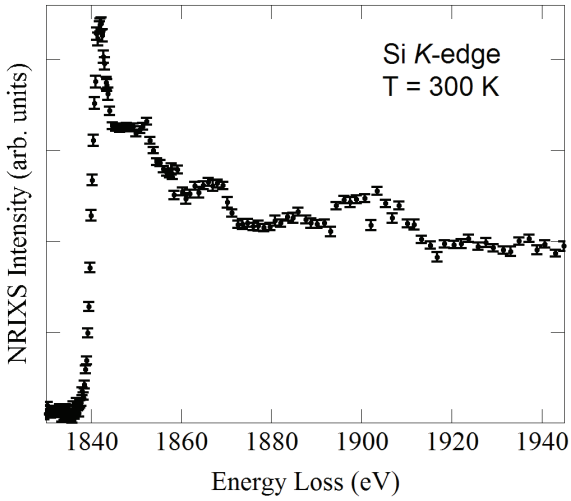

FIGURE 3. The 1*s* contribution to the NRIXS for pure Si. The errors due to Poisson statistics are approximately twice (three times) the size of the symbols in the near edge (extended) region and three The total measurement time for the data shown was ~2 hrs. The background (removed) is ~25% of the peak signal.

also makes possible measurements of edges with much higher binding energies. In Fig. 3, we present new measurements of NRIXS for the *K*-edge of pure Si. The initial state orbital is sufficiently small that all analyzers provide dipole-limited data and thus the counts from the different analyzers can be summed. We find good agreement between our Si *K*-edge results and prior soft x-ray measurements [30].

In conclusion, the lower energy resolution inelastic x-ray scattering (LERIX) spectrometer is now available for general users at the Advanced Photon Source. It is the first spectrometer specifically designed to optimize rapid measurement of the *q*-dependence of NRIXS from the core shells of light elements and the less tightly bound shells of heavier elements. Commissioning studies have demonstrated extremely low background counts, high sample throughput, and a wide range of applications for the user facility.

This work was supported by ONR Grant No. N00014-05-1-0843. PNC/XOR facilities at the Advanced Photon Source, and research at these facilities, are supported by the US DOE - Basic Energy Sciences, a major facilities access grant from NSERC, the University of Washington, Simon Fraser University, the Pacific Northwest National Laboratory and the Advanced Photon Source. Use of the Advanced Photon Source is also supported by the U.S. DOE, Office of Science, Office of Basic Energy Sciences, under Contract No. W-31-109-Eng-38.

REFERENCES

1. H. Nagasawa, *Journal de Physique* **48**, 863 (1987).
2. K. Tohji, Y. Udagawa, *Phys. Rev. B* **36**, 9410 (1987).
3. W. Schülke, A. Berthold, A. Kaprolat, and H. -J. Güntherodt, *Phys. Rev. Lett.* **60**, 2217 (1988).
4. T. Suzuki, A. Tanokura, N. Arimitsu, *J. Phys. Condens. Matter* **1**, 5187 (1989).
5. K. Tohji, Y. Udagawa, *Phys. Rev. B* **39**, 7590 (1989).
6. K. Tohji, Y. Udagawa, T. Matsushita, M. Nomura, T. Ishikawa, *J. Chem. Phys.* **92**, 3233 (1990).
7. N. Watanabe, H. Hayashi, Y. Udagawa, K. Takeshita, H. Kawata, *Appl. Phys. Lett.* **69**, 1370 (1996).
8. M. H. Krisch, F. Sette, C. Masciovecchio, and R. Verbeni, *Phys. Rev. Lett.* **78**, 2843 (1997).
9. H. Nagasawa, S. Mourikis, W. Schulke, *J. Phys. Soc. Japan* **66**, 3139 (1997).
10. Y. Udagawa, N. Watanabe, H. Hayashi, *J. de Physique IV* **7**, 347 (1997).
11. D. T. Bowron, M. H. Krisch, A. C. Barnes, *et al*., *Phys. Rev. B* **62**, 9223 (2000).
12. W. A. Caliebe, J. A. Soininen, E. L. Shirley, *et al*., *Phys. Rev. Lett.* **84**, 3907 (2000).
13. U. Bergmann, P. Wernet, P. Glatzel, *et al.*, *Phys. Rev. B* **66**, 092107 (2002).
14. K. Hämäläinen, S. Galambosi, J. A. Soininen, *et al*., *Phys. Rev. B* **65**, 155111 (2002).
15. W. Mao, H.K. Mao, P.J. Eng, *et al*., *Science* **302**, 425 (2003).
16. C. Sternemann, M. Volmer, J. A. Soininen, *et al*., *Phys. Rev. B* **68**, 035111 (2003).
17. U. Bergmann, H. Groenzin, O.C. Mullins, *et al*., *Petroleum Sci. Tech.* **22**, 863 (2004).
18. Y. Feng, G.T. Seidler, J.O. Cross, *et al., Phys. Rev. B* **69**, 125402 (2004).
19. P. Wernet, D. Nordlund, U. Bergmann, *et al*., *Science* **304**, 995 (2004).
20. Y. Meng, H.K. Mao, P.J. Eng, *et al*., *Nature Materials* **3**, 111 (2004).
21. D.A. Arms, T.J. Graber, A.T. Macrander, *et al*., *Phys. Rev. B* **71**, 233107 (2005).
22. S.K. Lee, P.J. Eng, H.K. Mao, *et al*., *Nature Materials* **4**, 851 (2005).
23. C. Sternemann, J. A. Soininen, S. Huotari, *et al*., *Phys. Rev. B* **72**, 035104 (2005).
24. P. Wernet, D. Testemale, J.L. Hazemann, *et al*., *J. Chem. Phys.* **123**, 154503 (2005).
25. C. Sternemann, J.A. Soininen, M. Volmer, *et al. J. Phys. Chem. Solids* **66**, 2277 (2005).
26. J.A. Soininen, A.L. Ankudinov, J.J. Rehr, *Phys. Rev. B* **72**, 045136 (2005).
27. T.T. Fister, G.T. Seidler, C. Hamner, *et al.*, in preparation.
28. T.T. Fister, G.T. Seidler, L. Wharton, *et al*., *Rev. Sci. Instrum.* **77**, 063901 (2006).
29. J.J. Rehr, J. Kozdon, J. Kas, *J. Synch. Rad.* **12**, 70 (2005), and references therein.
30. R. Sammynaiken, S. J. Naftel, and T. K. Sham, *et al*., *J. Appl. Phys.* **92**, 3000 (2002).